MODELING EDDY CURRENT INSPECTION OF A METALLIC SAMPLE WITH ROUND HOLE DEFECTS

Helena Geirinhas Ramos[1,2], *Artur Lopes Ribeiro*[1,2], *Dário Pasadas*[2], *Tiago Rocha*[2]

[1] Instituto Superior Técnico, Av. Rovisco Pais, 1049-001 Lisbon, Portugal, hgramos@ist.utl.pt
[2] Instituto de Telecomunicações, IST, Av. Rovisco Pais, 1, 1049-001, Lisbon, Portugal, arturlr@ist.utl.pt

Abstract: This paper presents a simple algorithm to model eddy current inspection when an uniform time-variable electric field in imposed in a region of a metallic plate sample with machined hole defects. The magnetic field perturbation due to a round hole defect subject to an unperturbed field is determined. The problem is formulated in terms of complex potentials and the method of conformal mapping is used to transform the domain with a round hole into a simpler domain in which the solution can be computed. To check the validity of this method the acquired voltage signals previewed with the algorithm are compared with data values measured using an experimental eddy current testing setup.

In addition to its great value in the design of non destructive testing instrumentation, optimum operating conditions and calibration methods, the algorithm described in this paper can constitute an important contribution to solve the inverse problem. The purpose of the inverse problem is to estimate the defect in the plate from measured data values. The measured data values include unknown measured noise that the inversion solution method amplifies and which can completely hide the physical solution corresponding to the noise free data. Thus an approach for the inverse problem solution from the accurate output results obtained with the purposed forward problem solver can be essential to the problem clarification.

Key words: conformal transformation; non-destructive evaluation; eddy current testing.

1. INTRODUCTION

Different methods of Non Destructive Testing (NDT) rely on the ability of operators to interpret the experimental data. Distractions such as boredom, poor visibility, inconvenient access to the evaluation screen or even lack of qualification, can increase the inspector decision error. An important aid in this area can be the use of automatic testing equipment and the technology involving the use of powerful processors for efficient understanding and interpretation of collected data which is rapidly evolving.

Eddy current testing (ECT) [1] is one of the methods that can be automated and computer controlled. An important advantage of this method is that there is no need of physical contact with the surface of the object under test and thus, the surface preparation is usually not necessary. In spite of its implementation simplicity, data produced by eddy current based equipment are among the most complicated to interpret and so the use of modeling techniques to predict the relationship between the defect size and the signal indicated in the detector are of great value. The integration of these modeling capabilities in a computer based device allows the choice of optimum operating parameters during the evaluation and gives insight to the collected data values [2].

This paper presents a simple algorithm to model eddy current inspection when a uniform time-variable magnetic field in imposed in a conductive sample with round hole defects [3-5]. It can be used to preview the acquired voltage signals using an experimental eddy current testing system. The study of round holes is an approach to pits due to corrosion in structural materials like aluminum alloys ot to fastener holes in airplanes junctions [6]. Furthermore the developed model can find application in the solution of the inverse problem which in this case consists of characterizing a defect by means of the magnetic field measurements. By using the noise free output data values from the model presented in this paper, the algorithm to solve the inversion problem can be tested without the corruption effect that comes out when measured raw data with small measurement errors are used instead.

2. SIMULATION MODEL

The paper describes a model to predict the surface electric and magnetic fields produced by a planar coil in a metallic plate that contains round hole defects. Let's assume that the planar coil produces in a limited area a uniform primary magnetic field that induces eddy currents in the sample surface that are also uniform in a limited area of the sample's surface when there are no defects or inhomogeneities present. Under these assumptions and neglecting the edge effect, one may conclude that the metal surface is charge free ($\rho = 0$) and the potential variation is restricted or confined to that given by Laplace's equation in that limited region [7]. The electric field, **E,** produced by the uniform magnetic field and the scalar potential, *V*, equations are respectively:

$$\mathbf{E} = -\nabla V = -\frac{\partial V}{\partial x}\mathbf{u}_x - \frac{\partial V}{\partial y}\mathbf{u}_y \tag{1}$$

$$\nabla^2 V = \frac{\partial^2 V}{\partial u^2} + \frac{\partial^2 V}{\partial u^2} = 0 \tag{2}$$

where $\mathbf{u}_x$ and $\mathbf{u}_y$ are the unit vectors.

The current density **J** is linearly related to the electric field:

$$\mathbf{J} = \sigma \mathbf{E} \tag{3}$$

being σ the material conductivity.

Thus, within this area with a Laplacian distribution for the potential the conformal mapping can be used to preview how a current line deviates from a hole.

2.1. Conformal mapping

To give an account of the problem consider the schematic diagram of the problem depicted in Fig. 1. Fig. 1(a) shows the geometric configuration of the current density and equipotentials in the presence of one round hole when an uniform magnetic field is imposed. The method of conformal mapping is going to be used to map this problem (geometric and boundary conditions) in a much simpler geometry as the one depicted in Fig. 1(b) in which the lines of force and the corresponding equipotentials are families of straight lines parallel to the axis. Within this simple geometry the problem can be more easily solved and afterwards the solution mapped back into the physical domain. Let the coordinate system be chosen so that its origin is on the upper boundary surface of the plate at the center of the round hole.

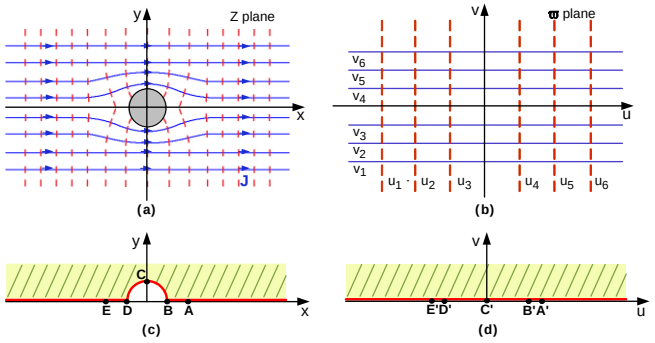

Fig. 1. Schematic of the problem.

To determine the perturbation of the current lines around the hole, a circle $x^2 + y^2 = 1$ is used to represent the hole in the conductive surface, and the lines of current distant from it are considered parallel to the *x* axis (Figs. 1(a) and 1(c)). Symmetry shows that part of the *x* axis exterior to the circle may be treated as a boundary, and so only the upper part of the plane is to be considered for the conformal transformation.

In a table of conformal transformations [8] one can find the function:

$$\varpi = \frac{1}{z} + z \tag{4}$$

where z is the normalized distance with *R* corresponding to the radius circle that represents the defect hole:

$$z = \frac{Z}{R} \tag{5}$$

The function (4) maps any point in the *z* plane specified by the coordinates *(x,y)* on a point in the ϖ plane defined by the coordinates *u(x,y)* and *v(x,y)*. The the upper semicircle and the parts of the *x* axis exterior to the circle, is mapped onto the entire *u* axis by the ϖ transformation. The region itself is mapped onto the upper half plane $v \geq 0$ (Fig. 1(d)). As depicted in Figs. 1.(c) and 1.(d), the *ABCDE* points represented in the *z* plane correspond the transformed points *A'B'C'D'E'* in the ϖ plane respectively.

On performing the ϖ transformation a new system of equipotentials and lines of force is obtain which also satisfy Laplace equations. The equipotential lines, that are represented as dotted lines in Fig. 1, are described in the *z* plane by curves:

$$u(x, y) = \text{const} \tag{6}$$

which correspond to straight lines drawn parallel to the imaginary axis in the ϖ plane. As (4) is conformal in the considered domain the angles are mapped faithfully, and since in the ϖ plane the straight lines $u = \text{const}$ and $v = \text{const}$ form a mesh which is orthogonal, the curves $v(x, y) = \text{const}$ always intersect the curves $u(x, y) = \text{const}$ perpendicularly. In other words, the curves $v(x, y) = \text{const}$ indicate the direction of the lines of force. To map back the solution in the physical domain, (1) must be inverted and as a result the equipotentials and lines of force are obtained in the *z* plane.

$$\bar{z}_{1,2} = \frac{w}{2} \pm \sqrt{\frac{w^2}{4} - 1} \tag{7}$$

The derivative of the analytic function, ϖ, is:

$$\frac{d\varpi}{dz} = \frac{d\varpi}{dx} = \frac{d\varpi}{d(jy)} \tag{8}$$

Writing (7) in more detail:

$$\frac{d\varpi}{dx} = \frac{\partial u}{\partial x} + j\frac{\partial v}{\partial x} \tag{9}$$

As (4) is analytic, then the real-value functions *u* and *v* are harmonic and the first order partial derivates of *u* and *v* verify the Cauchy-Riemann equations:

$$\frac{\partial u}{\partial x} = \frac{\partial v}{\partial y} \quad \wedge \quad \frac{\partial u}{\partial y} = -\frac{\partial v}{\partial x} \tag{10}$$

Considering *u* the potential function then the flux density is the complex conjugate of the derivative of ϖ and taking (3) the flux density can be considered the current density, **J**.

$$\sigma \left| \frac{d\varpi}{dz} \right|^* = \sigma \left[\frac{\partial u}{\partial x} + j\frac{\partial u}{\partial y} \right] = J_x + jJ_y \tag{11}$$

where:

$$\left| \frac{d\varpi}{dy} \right|^* = 1 - \frac{1}{z^2} = \frac{\left(x^2 + y^2\right)^2 - x^2 + y^2}{\left(x^2 + y^2\right)^2} - \frac{2xy}{\left(x^2 + y^2\right)^2} j \tag{12}$$

The lines of current deviating from the round hole obtained with (12) and the corresponding equipotentials lines are presented in Fig. 2.

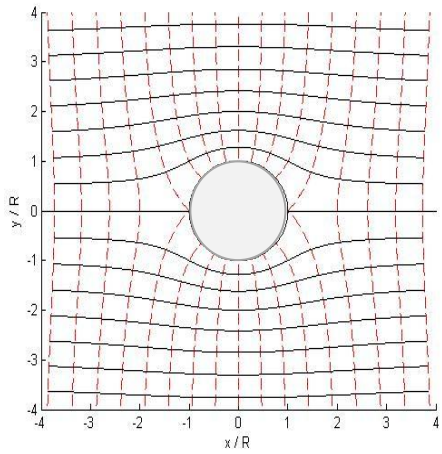

Fig. 2. Lines of current deviating from the hole (solid) and equipotentials (dotted) in the z plane.

In Fig. 3 the current density vector is depicted using the polar representation.

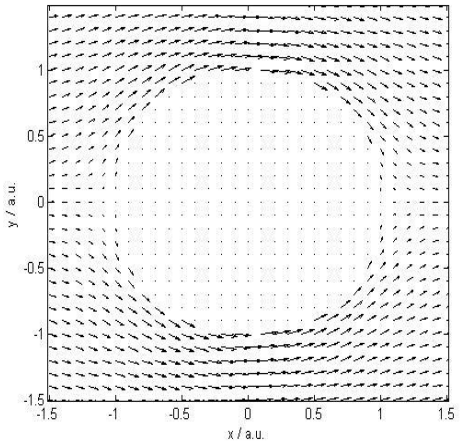

Fig. 3. Lines of current deviating from the hole.

The difference between the current density deviating from the hole that is presented in Fig. 3 and the unperturbed currents, is represented in Fig. 4 and corresponds to the perturbation of the current density originated by the defect. Thus, this current distribution can be considered the origin of the magnetic field perturbation resulting from the round hole existence.

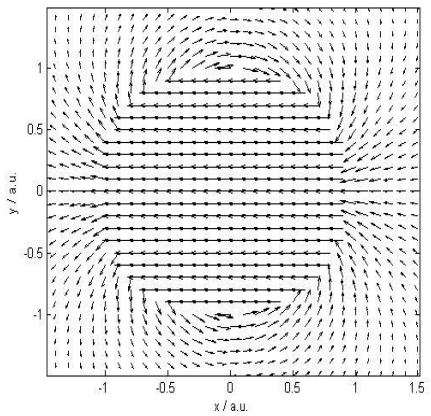

Fig. 4. Perturbation of the current density due to the hole.

2.1. Components of the magnetic field

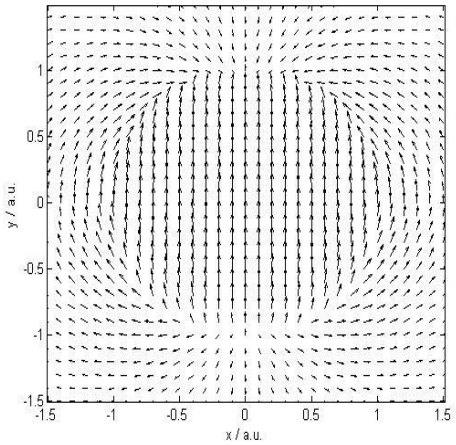

Fig. 5. Components of the magnetic field, H_x and H_y, in the (x,y) plane.

Fig. 5 represents the components of the magnetic field in the (*x*,*y*) plane and can be obtained from the current density depicted in Fig. 4 applying a discrete computation of the Biot-Savat law. To perform this calculus the *xy* plane is divided into cells and the magnetic field at the center of each cell is obtain iteratively by summing the contributions due to all the current element. Considering that the pair *(m,n)* references the position of each current element in the plate and the pair *(k,l)* the position of the point where the magnetic field is to be evaluated, the Biot-Savart law in the discrete form is:

$$\mathbf{H}(k,l) = \frac{1}{4\pi}\sum_{m,n}\frac{\mathbf{J}(m,n)\times\mathbf{R}^{k.l}_{m,n}}{R^2}\Delta V \qquad (13)$$

In (13), **R** represents the vector that connects the middle point of the cell where the magnetic field, **H**(*k*,*l*), is to be determined and the middle point of the cell where the current element, **J**(*m*,*n*), is located and ΔA the area of the unit element cell.

In Fig. 6 the surface of $H_y(x,y)$, representing the *y*-component of the magnetic field is depicted.

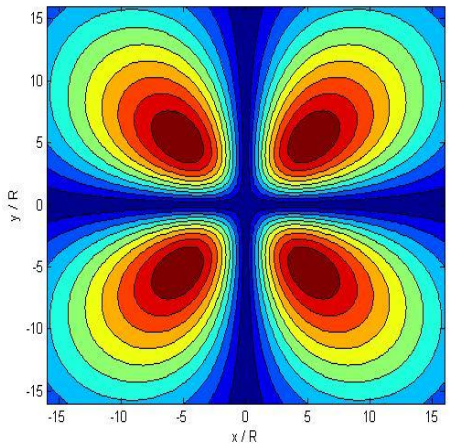

Fig. 6. Contour plot of the Hy component in the sample's surface simulated with the model.

In Fig. 7 the surface of $H_x(x,y)$, representing the *x*-component of the magnetic field is depicted.

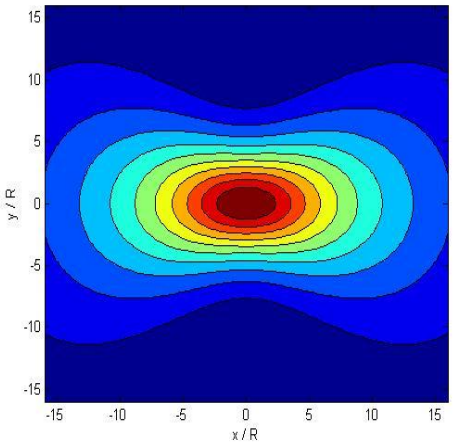

Fig. 7. Contour plot of the Hx component in the sample's surface simulated with the model.

3. EXPERIMENTAL WORK

3.1. Experimental setup

The experimental work was designed to provide data with which the results obtained from the model could be compared. Fig. 8 shows the block diagram of the system used in the experimental tests. The eddy current probe (ECP) is attached to a XY positioning system and contains a 50 turn planar excitation coil which generates in a rectangular area of approximately (25 x 20) mm^2 a uniform excitation magnetic field. The probe also includes a tiny (436x3370) μm magnetic sensor based on GMR (AA002-02 by Non Volatile Electronics) located in the coil plane in the center of the uniform magnetic field area with its sensible axis parallel to the *y* axis as presented in Fig. 6. The magnetic sensor has four giant magnetoresistors arranged in a Wheatstone bridge configuration and a permanent magnet biases the magnetic sensor to obtain a near linear response. A calibrator is used to inject a sinusoidal current with constant amplitude, I_{ex}=300 mA and f = 5 KHz, in the coil. The current is oriented in along the *y* direction in the vicinity of the upper surface of the aluminium plate and thus the resultant excitation magnetic field on ideal conditions is oriented along the *x* direction with a null component along the *y* direction.

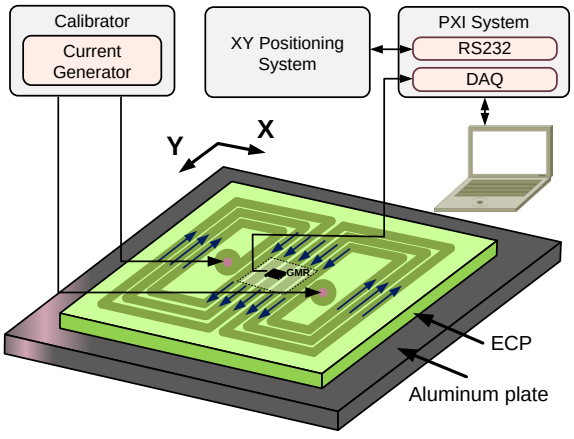

Fig.8. System block diagram.

The data acquisition module that acquires the signal waveform has 16 bit resolution and a maximum sampling frequency of 1 MS/s. It is assembled in a PXI system produced by National Instruments, which also includes a RS-232 interface to connect the motion controller of the XY positioning system. In the evaluated tests the positioning system had an adequate precision of 0.5 mm. A personal computer is used to control the PXI system and to process the obtained data.

3.1. Experimental results

In order to compare experimental data with the results obtained by simulation it is necessary to assure that the eddy currents being perturbed by the defect are enclosed within the uniform excitation magnetic field area. This condition imposes that the probe dimensions are scaled to the defects under study or more exactly to the area that limits the perturbed lines of current.

Fig. 9. presents the results obtained experimentally when a 1 mm thick aluminium plate with a 0.75 mm diameter hole is scanned. The area scanned by the probe was such that the eddy currents being perturbed by the presence of the hole were inside it.

The eddy currents induced by the excitation uniform magnetic field oriented along the *x*-direction are perturbed by the hole defect. The perturbation caused in the eddy currents generate a secondary magnetic field in the surface of the plate that is measured by the magnetic sensor. The *x*-direction primary magnetic field saturates the GMR sensor and therefore the GMR sensor is put orthogonally being only capable to measure the *y*-component of the resultant magnetic field. The experimental values obtained are shown in Fig. 9.

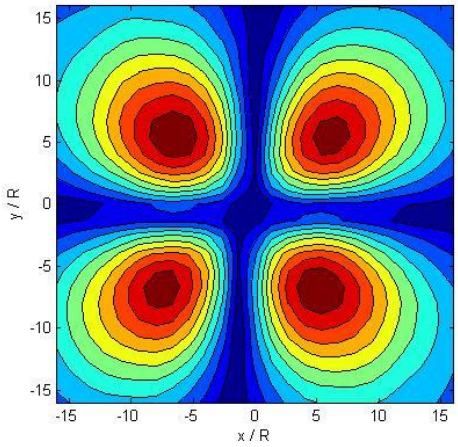

Fig. 9. Contour plot of the Hy component in the sample's surface from measured data values.

4. COMPARISON BETWEEN SIMULATED AND EXPERIMENTAL DATA VALUES

The spatial variation of the voltage detected by the eddy current probe when an aluminum plate with a round hole is scanned was presented in Fig. 9. A good agreement between the model results shown in Fig. 6. and the experimental data values is confirmed.

Fig. 10 shows the profile of $H_y(x,y)$ obtained with the model (solid line) and the measured values (asterisk) in a straight line containing the maximum values. The results have been adjusted for a liftoff (distance of the testing plate and the magnetic sensor of 0.9 mm [9].

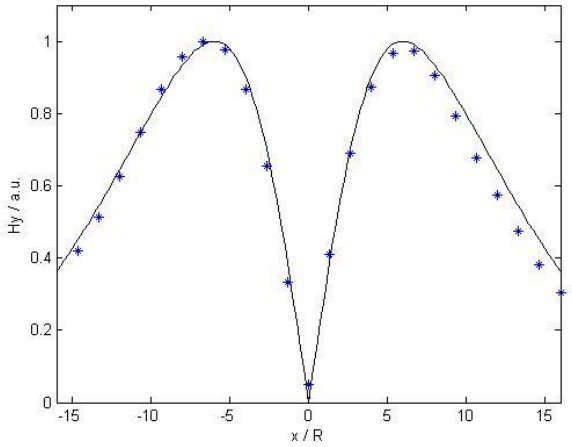

Fig. 10. Profile curves of the Hy component from model values (solid Line) and measured data values (asterisks).

A commercial 3D finite element model (FEM) simulation software package, Opera®, was used not only to validate the model based in the conformal transformation but also for other tasks involved within this research.

The current density distribution in the hole proximity is depicted in Fig. 11. As expected, it resembles the current density obtained from the model algorithm (Figs.2 nad 3). The current distribution was used to determine the dimensions of the probe and the area to be scanned.

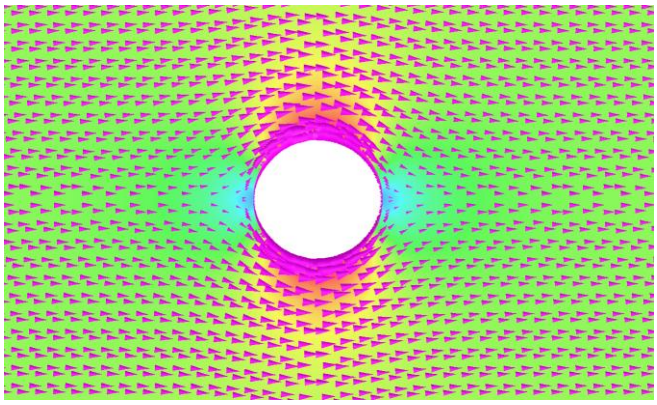

Fig. 11. Simulated superficial current density.

Fig. 12 depicts the y-component of the magnetic field obtained from the simulation software with uniform excitation field. These perturbations derive from a hole placed in the center of the test aluminum plate. These results are coherent with the Hy component from the proposed model.

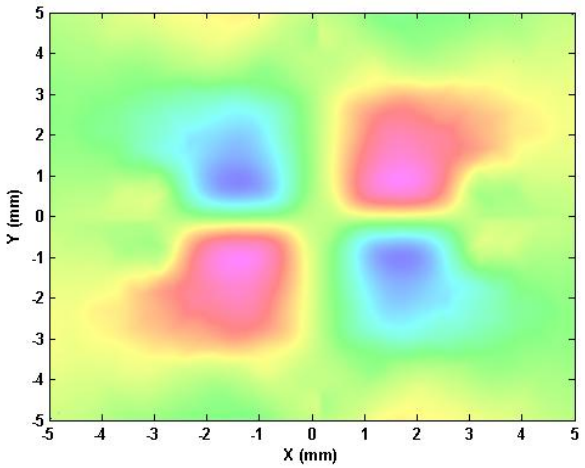

Fig. 8. Surface plot of the Hy component from simulated values.

4. CONCLUSION

This paper describes a simulation model based on a conformal transformation to preview the spatial variation of the voltage detected by an eddy current probe when an aluminum plate with a round hole is scanned. The simulation work was followed by a real experiment and the good agreement between both results allows us to conclude about the validity of the proposed method.

The problem is a simplification as the current density varies along the depth of the sample, nevertheless it can be a good approximation if the plate is thin when compared with the standard depth of penetration or the frequency high enough to produce strong shin effect in a very thin layer.

The modelling also helps to understand the interaction between the defect signal and the applied uniform field and due to its simplicity it can be used with advantage to generate data for the inversion of the defect signal problem solution testing.

AKNOWLEDMENTS

This work was supported by the Instituto de Telecomunicações – Project KeMaNDE and OMEGA. This support is gratefully acknowledged.

REFERENCES

[1] B. A. Auld and J. C. Moulder, “Review of advances in quantitative eddy current nondestructive evaluation”, J. Nondestr. Eval., vol. 18, no. 1, pp. 3-36, 1999.

[2] S. Sadeghi, D. Mirshekar-Syanhkal, “Scattering of an induced Surface Electromagnetic Field by Fatigue Cracks in Ferromagnetic Metals”, IEEE Trans. On Magn., Vol. 28, No.2, pp. 1008-1016, 1992

[3] A. Lopes Ribeiro, Luka Kufrin, H. G. Ramos, “Exploring the Eddy Current Excitation Invariance to Infer about Deffect Characteristics”, accepted for publication at the Review of Progress in Quantitative Nondestructive Evaluation (QNDE) da Springer. In press.

[4] A. Lopes Ribeiro, O. Postolache, H. M. Geirinhas Ramos “A Simple Forward Direct Problem Solver for Eddy Current Non-destructive Inspection of Aluminium Plates Using Uniform Field Probes”, Measurement Journal. Accepted for publication,, already available on-line.

[5] R. Clark and L.J. Bond, “Response of horizontal-axis eddy-current coils to layered media: a theoretical and experimental study“, IEE Proceedings, Vol. 137, Pt.A, No. 3, May 1990.

[6] Fredrik Lingvall, Tadeusz Stepinski “Automatic Detection of Defects in Riveted Lap-joints using Eddy Current”, ECNDT’98, September 1998, Vol.3, No.9, Sept. 98.

[7] Martin A. Plonus, Applied Electromagnetics, McGraw-Hill, New York,1978.

[8] R.V. Churchill, J.W. Brown, Complex Variables and Applications, fifthed., McGraw-Hill, 1990.

[9] A. Lopes Ribeiro, Francisco Alegria, O. Postolache, H. M. Geirinhas Ramos, “Liftoff Correction Based on the Spatial Spectral Behavior of Eddy Current Images”, IEEE Transactions on Instrumentation and Measurement, Vol. 59, No. 5, pp. 1362 - 1367, May, 2010.